Journal of Arid Environments 220 (2024) 105118

Contents lists available at ScienceDirect

Journal of Arid Environments

journal homepage: www.elsevier.com/locate/jaridenv

# The evolution of "Hot" droughts in Southern California, USA from the 20th to the 21st century

Peter T. Soulé [a,*], Paul A. Knapp [b]

[a] Appalachian Tree-Ring Lab, Department of Geography and Planning, Appalachian State University, Boone, NC, 28608, USA
[b] Carolina Tree-Ring Science Laboratory, Department of Geography, Environment, and Sustainability, University of North Carolina-Greensboro, Greensboro, NC, 27412, USA

ARTICLE INFO

*Keywords:*
Drought
Hot droughts
Southern California
USA
Palmer drought severity index
500 hPa geopotential height anomalies

ABSTRACT

Drought intensity and duration in southern California, USA during the 21st century has been exceptional, and the changing climate dynamics of drought in this arid and semiarid region have been linked to anthropogenic warming. We examine the frequency, intensity, and persistence of drought in southern California's two climatic divisions during 1900–2022 and use the monthly instrumental record of the Palmer Drought Severity Index (PDSI) to track how drought events have changed. We introduce an empirical definition of "hot drought" by combining mean summer PDSI values with standardized scores of mean summer minimum temperature. Droughts in southern California, USA have become increasingly more severe, frequent, and long-lived in the 21st century. Moderate drought conditions (PDSI $< -2$) were recorded during more than half of the months in the decade ending in 2020. Similarly, hot droughts, droughts associated with both water deficits and significantly above-normal temperatures, have become increasingly frequent in recent decades. By the 21st century, hot droughts were occurring in approximately half of the summers. Our findings support the idea that anthropogenic warming results in a changing drought climatology for arid and semiarid regions of southern California and that hot droughts will likely become the dominant drought type.

## 1. Introduction

The persistence and intensity of drought in southern California, USA during the 21st century have been unprecedented. Williams et al. (2022, p. 232) describe the 2000–2021 period as a "megadrought" in the southwestern United States and "the driest 22-yr period since at least 800". While the exceptionally wet winter of 2022–2023 returned soil moisture conditions to above normal in southern California, there are concerns that the processes controlling the spatiotemporal patterns of drought have changed due to human activities, such that we must now recognize the existence of "anthropogenic drought" (AghaKouchak et al., 2021). Indeed, Williams et al. (2020, p. 318) conclude that, in the absence of human influences, the 21st-century megadrought would likely not have been as extreme, and that future droughts may follow a trajectory of enhanced persistence and severity "relative to the range of natural multidecadal variability".

The idea that humans are changing drought dynamics through greenhouse gas-related warming was discussed in the early 21st century by Breshears et al. (2005, p. 15144) who called this evolving drought type a "global-change-type-drought". Similarly, Overpeck (2013, p. 350) editorialized on how anthropogenic changes are contributing to drought enhancement in North America and described these as "hot droughts". While hot droughts could be defined in various ways using either instrumental measurements of temperature and precipitation or drought indices derived from empirical measurements, the general idea is that the water demand (i.e., evapotranspiration) increases beyond the normal supply from precipitation in association with above-normal temperature, creating deficits in soil moisture that in turn negatively impact ecosystems processes, agriculture, and a suite of human activities. For example, flows in the Colorado River in the 21st century were reduced by 19% in association with an extended hot drought (Udall and Overpeck 2017) and Fettig et al. (2019) report extensive (e.g., 46% in lower elevations and 60% in higher elevations) tree mortality in their central and southern Sierra Nevada, California study sites following the severe drought of 2012–2015. Cheng et al. (2019) demonstrate through a modeling approach that the processes driving hot droughts can include positive feedbacks, such that extended heat waves in the southwestern United States create upward fluxes of sensible heat that further enhance

* Corresponding author. Department of Geography and Planning, Appalachian State University, Boone, NC, 28608, USA.
*E-mail address:* soulept@appstate.edu (P.T. Soulé).

https://doi.org/10.1016/j.jaridenv.2023.105118
Received 21 September 2023; Received in revised form 2 November 2023; Accepted 4 December 2023
0140-1963/© 2023 Elsevier Ltd. All rights reserved.

surface rates of evapotranspiration. Similar processes have been identified in Europe during extreme summer droughts of the 21st century (Teuling 2018), and drought events in China have increased since the mid-20th century in the absence of any significant changes in precipitation, leading to the conclusion that anthropogenic warming is driving a changed climate where hot droughts are more prevalent (Chen and Sun 2017).

Drought in western North America (e.g., Stahle et al., 2007), and California specifically (e.g., Williams et al., 2015), is a natural component of our climate system. Tree-ring-based analyses extend our record of drought in southern California to 800 CE (e.g., Robeson 2015) and can be used to place more recent droughts into a historical climatic perspective. Megadroughts — droughts that are significant in terms of both intensity and multi-decadal duration — have occurred multiple times in the proxy-reconstructed record (Williams et al., 2020). Droughts of this intensity and longevity in modern times produce a suite of significant and negative impacts on human activities, including food insecurity, increased wildfire intensity, reduced water supply, air-quality issues, and decreased water quality for fisheries (Swain et al., 2014). Within ecosystems, megadroughts can result in widespread die-off of vegetation and create substantive changes in the structure and function of forest ecosystems through post-drought effects or "drought legacies" whereby current drought impacts manifest in negative impacts during future droughts (Müller and Bahn 2022, p. 5086). If the spatio-temporal patterns and driving processes of drought are undergoing substantive changes within a region as ecologically sensitive and densely populated as southern California, this raises concerns about how such changes may vector in the future.

Here we examine temporal patterns of drought frequency, intensity, and persistence in two climatologically distinct (one largely arid, one largely semiarid) climatic divisions of southern California using the instrumental data record of the 20th and 21st centuries. We document how the dynamics of drought have changed temporally in association with anthropogenic warming through an analysis of summer drought conditions that includes an empirical definition of "hot drought" incorporating both drought intensity and temperature anomalies.

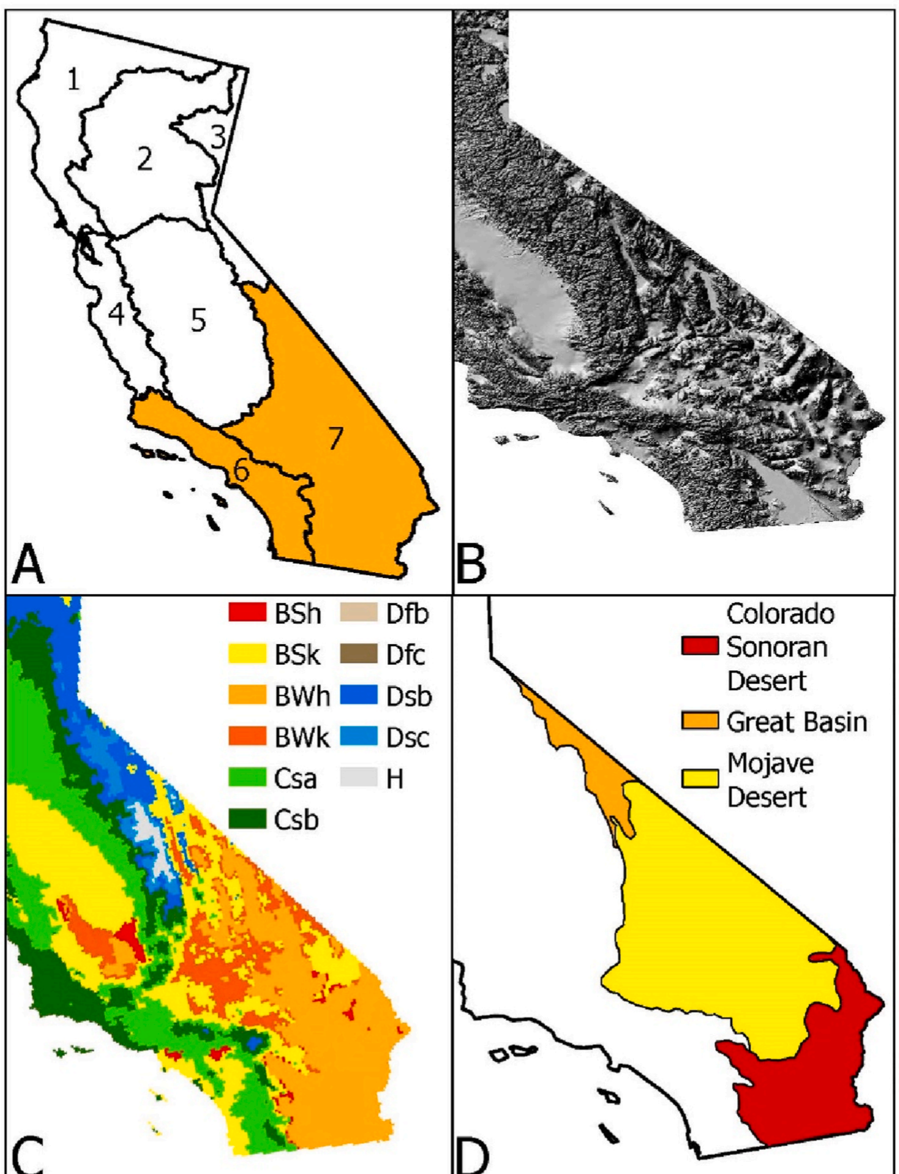


**Fig. 1.** Study area showing climatic division boundaries in California (A, public domain data source https://psl.noaa.gov/data/usclimdivs/boundaries.html), digital elevation model (B), Koppen climate types (C, public domain data source https://hub.arcgis.com/documents/a1209a5383c04ef18addea0e10ab10e5/about), and major deserts (D, public domain data source Deserts: https://water.usgs.gov/GIS/metadata/usgswrd/XML/sir045205_deserts_sw.xml).

Additionally, we examine patterns of upper-level (500 hPa geopotential heights) flow for summer droughts to determine how the broad-scale forcing mechanisms are influencing the surface patterns.

## 2. Materials and methods

### 2.1. Study area and climate classification

We used Palmer Drought Severity Index (PDSI; Palmer, 1965) data from the South Coast Drainage (hereafter CD6) and Southeast Desert Basins (hereafter CD7) Climate Divisions of California (Fig. 1) to characterize long-term drought conditions. These two climatic divisions range from 32 to 35 °N (CD6) and 32–37 °N (CD7) and cover all southern California from the Pacific Ocean to the Arizona and Nevada borders, and for CD7 is comprised of the Mojave, Colorado/Sonoran, and Great Basin Desert regions (Kauffman, 2003). Both climatic divisions are topographically diverse with elevations ranging from sea level (or less) to mountain ranges with peaks over 3500 m. Comprising a population of approximately 22 million (US Census Bureau, 2022) the study area includes the major population centers of Los Angeles (3,822,238), San Diego (1,381,362), Anaheim (344,461), and Riverside (320,764) (https://www.california-demographics.com/cities_by_population).

Using the Köppen system (http://www.meteotemplate.com/template/plugins/climateClassification/koppen.php), CD6 (Fig. 1) is predominantly classified as a Hot Summer Mediterranean climate (Csa) characterized by hot, dry summers and mild, wetter winters (Figs. 1c and 2a). The majority of CD7 classifies as a Hot Desert Climate (BWh, Fig. 1c) and displays a similar annual pattern of temperature and precipitation, but with less annual precipitation (155 mm) than CD6 (439 mm) and more extreme summer temperature (maximum temperatures of 35 °C versus 30 °C; Fig. 2b). While similar in terms of the annual progression of heat and moisture, the regions encompassing CD6 and CD7 are climatologically distinct and spatially expansive, thus providing for an excellent geographic representation of arid and semiarid climates of the southwestern United States. Summer aridity in CD6 and CD7 is caused by the influence of the stable, eastern side of the North Pacific High, while a winter maximum of precipitation is delivered principally from mid-latitude wave cyclones. Precipitation is less in CD7 due to a combination of rainshadow effects and continentality.

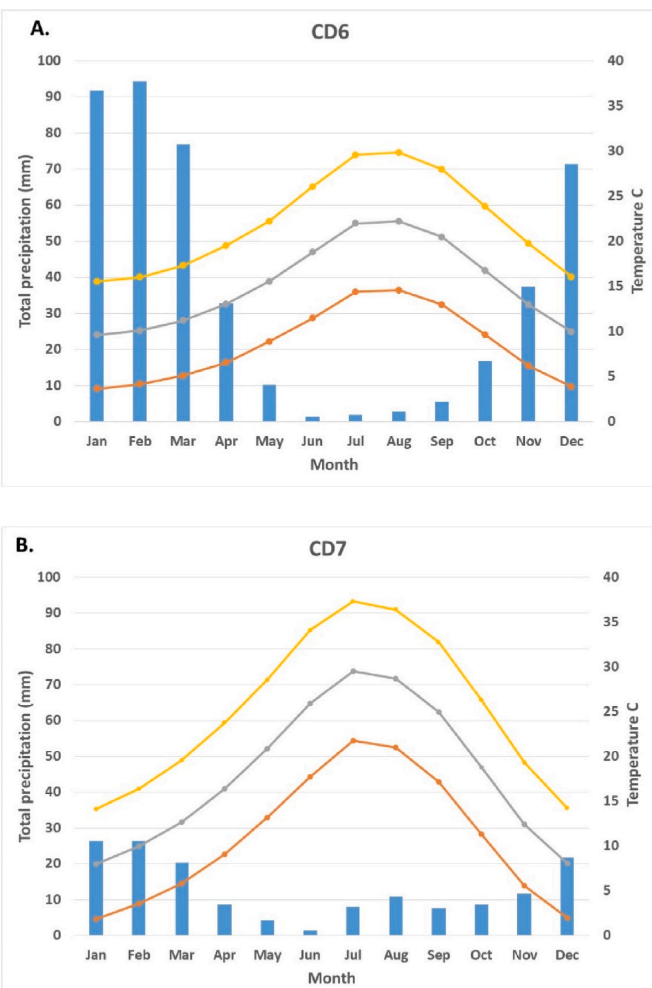


**Fig. 2.** Climographs showing mean monthly total precipitation (vertical bars) and mean monthly minimum, maximum, and mean temperatures (lines) for CD6 (A) and CD7 (B). Observations are from 1901 to 2022.

### 2.2. PDSI data

The PDSI is referred to as a measurement of "meteorological" drought as it is faster to respond to inputs of precipitation than the Palmer Hydrological Drought Index and slower than the Palmer Z-Index (https://www.ncei.noaa.gov/access/monitoring/historical-palmers/overview). The Palmer indices consider both the meteorological supply of moisture via monthly precipitation and the demand (i.e., evapotranspiration) based largely on temperature (Palmer 1965; Soulé 1992). PDSI values for any given month are water-balanced based, account for antecedent soil moisture conditions, and ultimately are designed to reflect deviations from mean climatic conditions for specific regions and their climate types (Palmer 1965). The PDSI is centered on zero (near-normal), with negative values of the index reflecting moisture deficits or drought, and positive values representing above-normal moisture (Palmer 1965). The larger the absolute value of the index, the more extreme the drought (wetness). The PDSI is a frequently used metric for characterization of regional climatic conditions (e.g., Aiken and Rauscher 2020), and is used in tree-ring research in climate/growth analyses (e.g., Liu et al., 2017). Bias-corrected values of the PDSI are available monthly back to 1895 from NOAA's Physical Science Laboratory (https://psl.noaa.gov/data/timeseries/).

We used a 122-year record of the PDSI (1901–2022) as that allowed for the calculation of drought conditions for four 30-year climatic normal periods aligned with those calculated by the National Oceanic and Atmospheric Administration (NOAA; e.g., 1991–2020; https://www.ncei.noaa.gov/products/land-based-station/us-climate-normals periods). We followed the methods first outlined by Diaz (1983) and defined a drought event as any period with three or more consecutive months with PDSI values $< -2$ (qualitatively "moderate drought" per Palmer 1965). We tabulated the number of drought events for the 30-year periods 1901–1930, 1931–1960, 1961–1990, and 1991–2020. We calculated the mean monthly length and mean severity of drought events for these four 30-year periods. We also counted the number of months per year with PDSI $< -2$ annually and then tabulated these by decade and for the 30-year periods. We tested for long-term (1901–2020) trends in the decadally-averaged number of drought events using Kendall's Tau-B ($\tau_b$).

### 2.3. Summer drought, hot summer drought, and 500 hPa geopotential height anomalies

We based the occurrence of summer (i.e., June–August) drought (SD) and "hot" summer drought (HSD) on mean summer PDSI values, and additionally for HSDs, mean summer minimum temperatures (obtained from: https://psl.noaa.gov/cgi-bin/data/timeseries/timeseries1.pl), from CD6 and CD 7 for the period 1901–2022. We tested for long-term (1901–2022) trends in mean summer PDSI values and mean summer minimum temperatures using Kendall's Tau-B. We defined a SD as any year with a mean summer PDSI $< -2$ and a HSD as any summer with both a mean summer PDSI $< -2$ and a mean minimum temperature standardized score (i.e., z-score) > 1, which is 1.1 °C above the mean for both CD6 and CD7. We used minimum temperatures as the 1901–2022 trend was greater than for maximum temperatures by approximately 0.55 °C/century and thus, exceptionally warm (i.e., "hot") summers were better identified using this metric. We determined mean drought severity between SD and HSD years using an independent samples difference of means *t*-test. To evaluate the meteorological forcing mechanisms associated with drought in southern California, we examined 500 hPa geopotential height anomalies and surface temperature anomalies concurrent with the ten most extreme SD years and ten most extreme HSD years, both defined by the lowest mean summer PDSI values. We mapped the upper-level and surface temperature anomalies using the NCEP/NCAR Reanalysis Program (data available from 1948 to 2022; https://psl.noaa.gov/cgi-bin/data/composites/). This period excluded only one SD (1934, CD7) and we replaced that year with the next-most severe drought (2004).

## 3. Results

### 3.1. Drought conditions by 30-year climatic normal periods

The most dramatic finding from the 30-year climatic normal period analyses of drought is the number of months when PDSI values are $< -2$ (moderate drought or worse; Table 1). For CD6, 8.9% of the months in the first 30-year period of the 20th century reached this threshold, but by the 1991–2020 period that had increased to 43.6%. While the desert climate of CD7 is comparatively more drought-prone than the Mediterranean climate of CD6, the number of months with moderate drought increased from 15.3% to 52.2%. While the other drought metrics did not always increase with each 30-year interval, they are generally increasing, such that by the 21st century droughts in southern California are occurring more frequently, at greater severity, and are lasting longer in comparison to early 20th century droughts. We found similar patterns of drought frequency when evaluating the data in decadal units (Fig. 3), with the number of months experiencing either moderate drought conditions or worse increasing from a low of 2.5% in the decade ending in 1910 to a high of 65.8% in the decade ending in 2020 for CD6 and from 0% in the decade ending in 1920 to 56.7% in the decade ending in 2020 for CD7. We found significant ($p < 0.001$) positive trends in the number of months with PDSI values $< -2$ per decade for both CD6 ($\tau_b = 0.72$) and CD7 ($\tau_b = 0.75$).

### 3.2. Summer droughts and "hot" summer droughts

In both CD6 and CD7, SDs are more likely to occur than HSDs (Fig. 4). For CD6, the combined count of SDs ($n = 24$) and HSDs ($n = 13$) was 37 with 10 (77%) HSDs recorded since 2000. In CD7 droughts occurred more frequently ($n = 48$, 29 SDs and 19 HSDs) with 13 (68.4%) of the HSDs occurring in the 21st century. In both CD6 and CD7, the first HSD was not recorded until 1959, and the increasing frequency of HSDs

**Table 1**
Characterization of drought in CD6 (boldfaced and italicized) and CD7, 1901–2020 by 30-year climatic normal periods.

| 30-year period | # months PDSI < −2 | # drought events | mean length drought events(# months) | mean severity drought events | longest drought event (# months) |
|---|---|---|---|---|---|
| 1901–1930 | 32 | 3 | 7.3 | −2.33 | 16 |
| 1901–1930 | 55 | 5 | 9.8 | −2.44 | 16 |
| 1931–1960 | 58 | 5 | 10.8 | −2.8 | 20 |
| 1931–1960 | 77 | 7 | 10.6 | −2.92 | 17 |
| 1961–1990 | 112 | 15 | 7.3 | −3.03 | 24 |
| 1961–1990 | 122 | 12 | 9.5 | −2.68 | 24 |
| 1991–2020 | 157 | 7 | 20.4 | −4.13 | 55 |
| 1991–2020 | 188 | 13 | 13 | −3.06 | 31 |

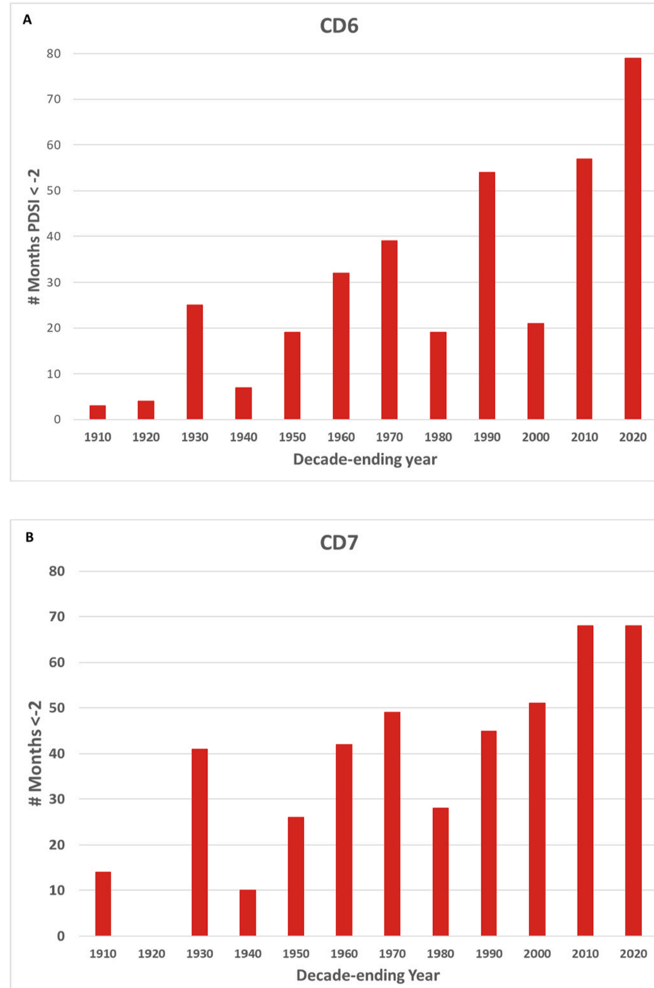


**Fig. 3.** The number of months per decade (e.g., 1901–1910) with PDSI values $< -2$ for CD6 (A) and CD7 (B) during 1900–2020.

is concurrent with the increasing trend of summer temperature (Fig. 4). HSDs were more severe (i.e., more negative PDSI values) than SDs for both regions. For CD6, mean PDSI values (−5.32) for HSD years were significantly ($p < 0.01$) less than mean PDSI values (−3.47) for SD years. Similarly, for CD7 mean PDSI values (−3.46) for HSD years were significantly ($p < 0.01$) less than mean PDSI values (−2.81) for SD years. We found significant negative (i.e., indicating worse drought severity, $p < 0.001$) long-term trends in mean summer PDSI values for CD6 ($\tau_b = -0.32$) and CD7 ($\tau_b = -0.23$). Long-term trends in mean summer minimum temperatures were positive, stronger (CD 6 $\tau_b = 0.53$; CD7 $\tau_b = 0.46$) and significant ($p < 0.001$).

### 3.3. Upper-level height and surface temperature anomalies for SDs and HSDs

For the 10 most-intense SD years for CD6, the upper-level anomaly pattern is distinctly different from that experienced during HSD years (Fig. 5). There is enhanced ridging in northwestern Canada with the axis peak centered approximately 2800 km north of southern California and an enhanced summertime Aleutian low. The strong Aleutian low and negative height anomalies over the Pacific serve to enhance onshore flow into southern California, resulting in cooler temperatures relative to HSD years. Surface air temperature anomalies in southern California during SD years were near-average (z-score = 0.1).

Upper-level (500 hPa) summer temperature anomalies during HSDs in CD6 are dominated by above-average heights in the northwestern

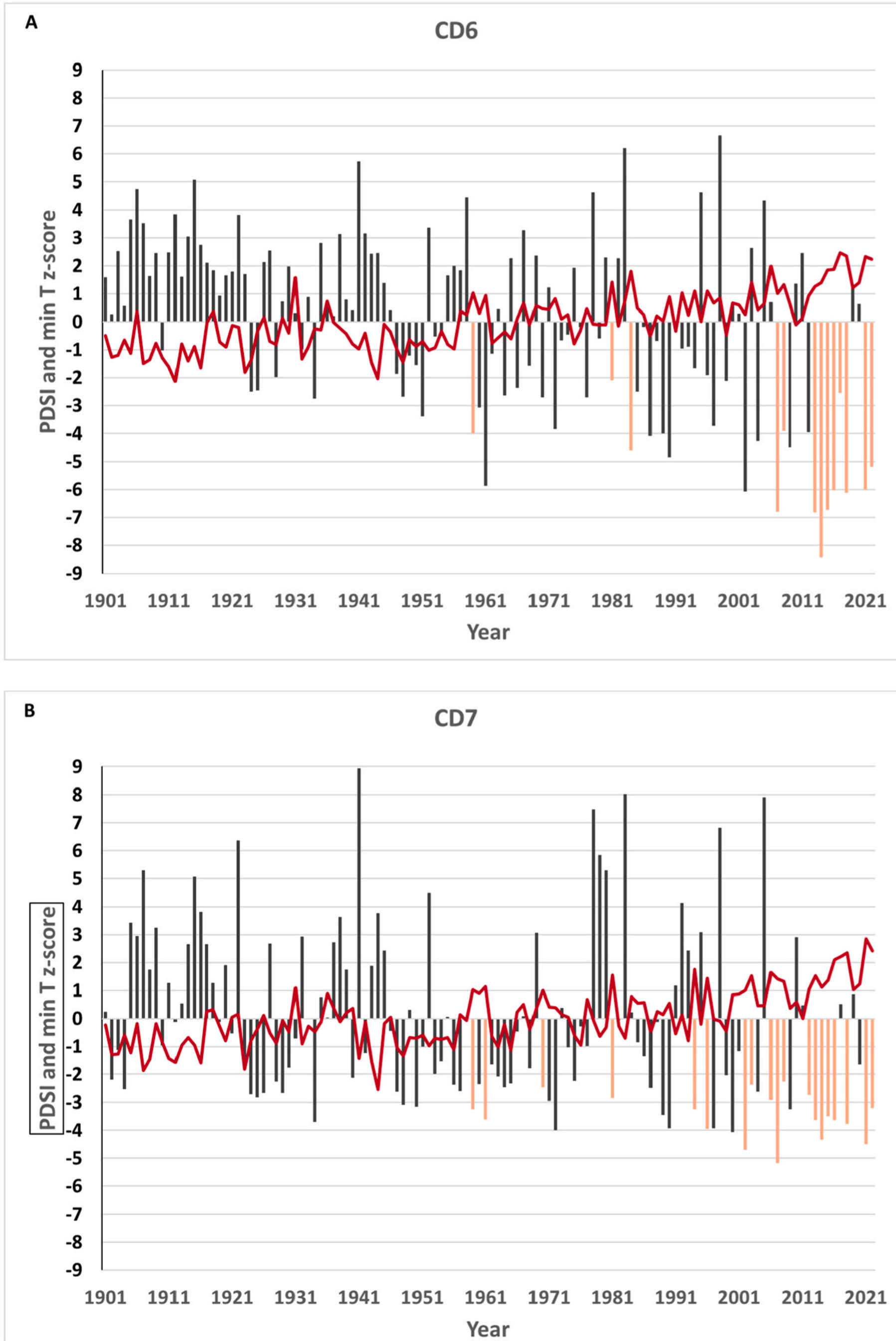


**Fig. 4.** Mean summer (JJA) PSDI values (either black bars or rose bars for HSD years) and mean of summer minimum temperature standardized scores (red line) for CD6 (A) and CD7 (B), 1901–2022.

United States, with the core anomalies centered in the northern Rocky Mountains, USA (Fig. 5). In turn, the pattern of ridging results in subsidence, clear skies, and positive surface temperature anomalies in the same region. While the ridge axis is approximately 1600 km northeast of southern California, this atmospheric pattern would reduce the influx of moisture into CD6 from the Pacific Ocean. The frequency of offshore flow under high pressure conditions is conducive for the formation of HSDs (i.e., low moisture and high temperature).

CD6 and CD7 share six of the same ten most extreme HSD years, thus the upper-level and surface temperature anomaly patterns during HSDs for CD7 (Fig. 6) are similar to those for CD6 (Fig. 5), with enhanced western ridging resulting in broad-scale positive surface temperature anomalies. For CD7 summer drought years, there is also enhanced ridging in northwestern Canada but the summertime height anomaly over the Aleutian Islands regions is not as extreme as for SD years for CD6. Temperature anomalies over southern California are largely neutral.

## 4. Summary and conclusions

Analyses of the frequency, intensity, and severity of drought in the United States are common in the climatic literature (e.g., Karl 1983; Soulé 1992; Strzepek et al., 2010; Chiang et al., 2021). While our analyses show that droughts in southern California have become more severe, are occurring more frequently, and are of longer duration in the 21st century (Table 1, Figs. 3 and 4), other areas of the United States

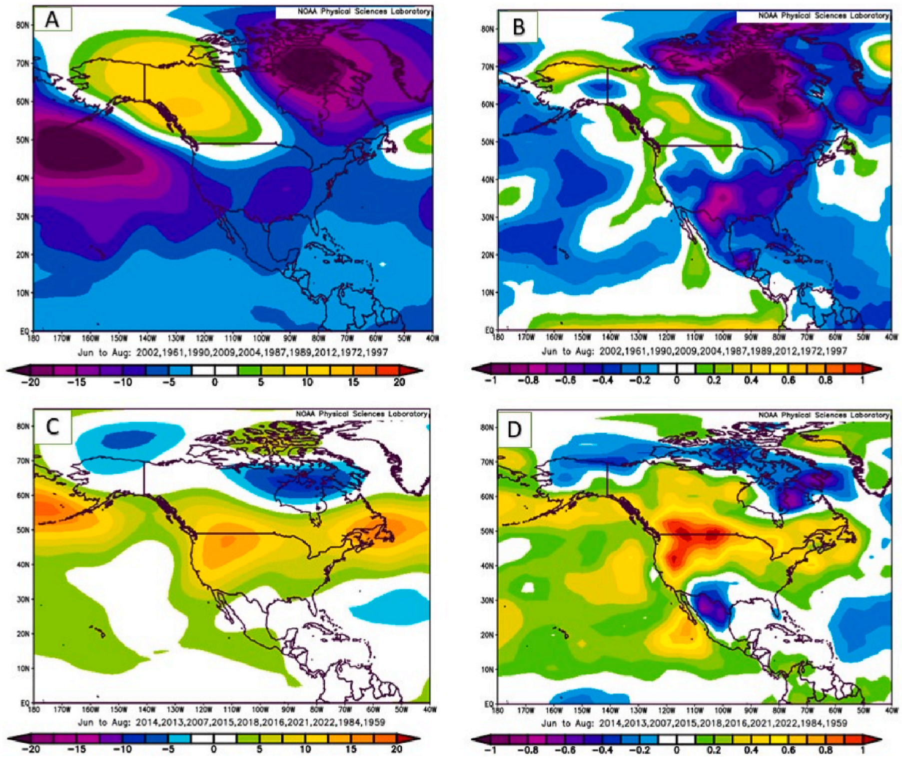


**Fig. 5.** A) 500 hPa height (DM) and B) surface temperature (°C) anomalies for the 10 SD years (1948–2022) with the lowest PDSI values for CD6. C) 500 hPa height (DM) and D) surface temperature (°C) anomalies for the 10 HSD years (1948–2022) with the lowest PDSI values for CD6. The years are listed beginning with the lowest summer mean PDSI values.

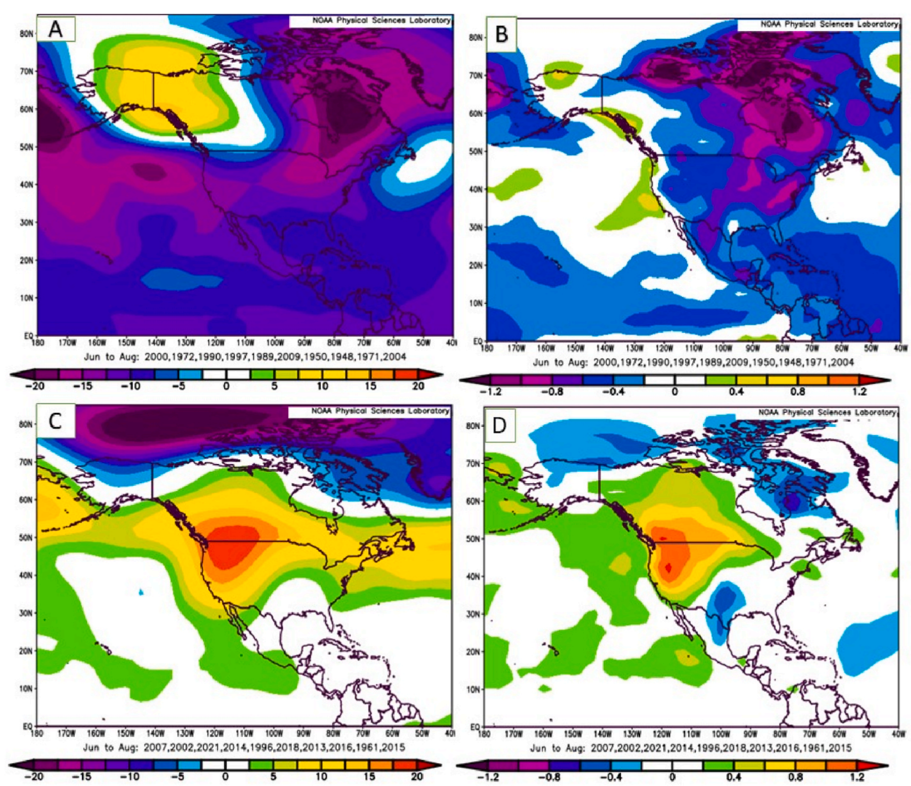


**Fig. 6.** A) 500 hPa height (DM) and B) surface temperature (°C) anomalies for the 10 SD years (1948–2022) with the lowest PDSI values for CD7. C) 500 hPa height (DM) and D) surface temperature (°C) anomalies for the 10 HSD years (1948–2022) with the lowest PDSI values for CD7. The years are listed beginning with the lowest summer mean PDSI values.

have experienced extreme drought conditions prior to anthropogenic warming. For example, the areal coverage of moderate or worse (PDSI < −2) drought-affected land in the United States circa 2005 was similar to that observed in 1955 and 1935 (approximately 30%; Heim 2017), and drought conditions (PDSI < −2) in the 1930s in central Kansas persisted for 63 consecutive months with a mean PDSI intensity of −4.2. Thus, while long-duration and high-intensity droughts have always been a part of regional climates in the United States, in southern California the contrasts between the early decades of the 20th and 21st centuries are extreme and concur with global observations of increasing frequency, intensity, and duration of droughts associated with anthropogenic forcing (Chiang et al., 2021). For CD6, the number of months with PDSI values < −2 had a 4.9-fold increase from the first (1901–1930) climatic normal period to the last (1991–2020), and in CD7 more than half of the months experienced moderate drought conditions or worse by the 1991–2020 period (Table 1). While droughts are, by nature, typically persistent and long-lived climatic events, there was also an extreme temporal evolution, as the longest droughts recorded using the threshold of three or more consecutive months with PDSI < −2 increased by 39 months for CD6, and by 15 months for CD7 from the first to the last 30-year climatic normal periods. The longest recorded drought event in southern California's CD6 lasted 4.6 years, (June 2012–December 2016). In contrast, the longest drought in the 20th century in southern California was two years (March 1989–February 1991) for both CD6 and CD7.

### 4.1. Drivers of hot droughts and temporal evolution

The evolution of HSD frequency is concurrent with a long-term warming trend in southern California that initiated in the late 1970s with a marked increase beginning in the 2010s. Upper-level synoptic conditions during the latter period were characterized by a strong wintertime anticyclonic circulation pattern centered in the Northeast Pacific informally identified as the "Ridiculously Resilient Ridge" (Swain et al., 2017, p.12194). During these years, which promoted the antecedent conditions for summer drought, the anticyclone weakened during the spring with a development of summertime high pressure centered over the Northern Rockies of the USA and Canada similar to the pattern shown in Fig. 5a and 6a. Explanations for wintertime ridge formation include increased jet stream waviness and persistence associated with reduced Arctic Sea ice extent (ASIE) and Arctic amplification (AA; e.g., Francis and Vavrus, 2012, 2015; Cvijanovic et al., 2017) and internal climatic variability via the influence of Pacific Ocean temperature anomalies (e.g., Swain et al., 2017).

AA also likely affects summer circulation patterns (Coumou et al., 2018) that have favored warmer and drier conditions in California. Since the 1980s, weakened summertime polar jet stream activity associated with warmer Arctic temperatures and reduced ASIE has affected mid-latitude North American circulation patterns (Wu et al., 2023). Decreased ASIE reduces the temperature contrast between high and mid-latitude regions resulting in a slower and meridionally amplified jet stream that is more prone to becoming spatiotemporally persistent (Francis and Vavrus, 2021). In western North America, the persistence of quasi-stationary ridges has promoted warmer and drier conditions linked with increased fire activity (Knapp and Soulé, 2017, Jain and Flannigan 2021; Zou et al., 2021). We also find empirical evidence of a link between reduced ASIE (https://nsidc.org/arcticseaicenews/sea-ice-tools/) in late winter/early spring (mean February–April) and minimum temperature during June–August for both CD6 ($r$ = -0.65, $p < 0.01$) and CD7 ($r$ = -0.70, $p < 0.01$) during 1979–2022 suggesting a lagged effect on summertime temperature may contribute to the occurrence of HSDs.

The vectors we observed for droughts and HSDs in southern California (i.e., increased frequency, severity, and persistence) in recent decades do not guarantee the trends will continue through the third decade of the 21st century and beyond. While Wang et al. (2022) suggest that HSDs will become even more frequent due to the impacts on upper-level flow from AA/ASIE loss, Deser et al. (2014) and Screen et al. (2014) argue that internal, or non-anthropogenic, climate variability makes this difficult to predict, and is complicated when 40–60% of the total uncertainty of ASIE projections is associated with internal variability (Bonan et al., 2021). However, our results suggest that anthropogenic drought (AghaKouchak et al., 2021) must now be recognized as a potential feature of the climatology of southern California, and we must plan accordingly for a future where extended periods of extreme moisture deficits may continue to occur.

## CRediT authorship contribution statement

**Peter T. Soulé:** Conceptualization, Methodology, Validation, Formal analysis, Investigation, Resources, Data curation, Writing – original draft, Writing – review & editing, Visualization, Supervision, Project administration, Funding acquisition. **Paul A. Knapp:** Conceptualization, Methodology, Validation, Formal analysis, Investigation, Resources, Writing – review & editing, Visualization, Supervision, Funding acquisition.

## Declaration of competing interest

The authors declare that they have no known competing financial interests or personal relationships that could have appeared to influence the work reported in this paper.

## Data availability

Data will be made available on request.

## Acknowledgments

We thank the University Research Council at Appalachian State University and the University of North Carolina Greensboro for providing internal funding to support this project. We thank Ken Kietzer of the California State Parks system for helping facilitate the permitting process. We thank Stephen James and other staff at the Mount San Jacinto State Park Ranger Station for providing helpful information on climatic conditions and forest ecosystems in the park. We thank Tim Jones of the Palm Springs Aerial Tramway for providing complimentary transport to the state park for our research team. We thank Gabe Small at the University of North Carolina Greensboro for cartographic assistance.

## References

Aiken, Emily K., Rauscher, Sara A., 2020. Evaluation of the climate extremes index over the United States using 20th and mid-21st century north American regional climate change assessment Program data. Int. J. Climatol. 40 (3), 1542–1560.

AghaKouchak, Amir, Ali, Mirchi, Madani, Kaveh, Di Baldassarre, Giuliano, Ali, Nazemi, Alborzi, Aneseh, Hassan, Anjileli, et al., 2021. Anthropogenic drought: definition, challenges, and opportunities. Rev. Geophys. https://doi.org/10.1029/2019RG00068e2019RG000683.

Bonan, David B., Lehner, Flavio, Holland, Marika M., 2021. Partitioning uncertainty in projections of Arctic sea ice. Environ. Res. Lett. 16 (4), 044002.

Breshears, David D., Neil, S. Cobb, Paul, M. Rich, Kevin, P. Price, Craig, D. Allen, Balice, Randy G., Romme, William H., et al., 2005. Regional vegetation die-off in response to global-change-type drought. Proc. Natl. Acad. Sci. USA 102 (42), 15144–15148.

Chen, Huopo, Sun, Jianqi, 2017. Anthropogenic warming has caused hot droughts more frequently in China. J. Hydrol. 544, 306–318.

Cheng, Linyin, Martin, Hoerling, Liu, Zhiyong, Eischeid, Jon, 2019. Physical understanding of human-induced changes in US hot droughts using equilibrium climate simulations. J. Clim. 32 (14), 4431–4443.

Chiang, Felicia, Mazdiyasni, Omid, AghaKouchak, Amir, 2021. Evidence of anthropogenic impacts on global drought frequency, duration, and intensity. Nat. Commun. 12 (1), 2754.

Coumou, Dim, Di Capua, Giorgia, Vavrus, Steve, Wang, Lei, Wang, Simon, 2018. The influence of Arctic amplification on mid-latitude summer circulation. Nat. Commun. 9 (1), 2959.

Cvijanovic, Ivana, Santer, Benjamin D., Bonfils, Céline, Lucas, Donald D., Chiang, John CH., Zimmerman, Susan, 2017. Future loss of Arctic sea-ice cover could drive a substantial decrease in California's rainfall. Nat. Commun. 8 (1), 1947.
Deser, Clara, Phillips, Adam S., Alexander, Michael A., Smoliak, Brian V., 2014. Projecting North American climate over the next 50 years: uncertainty due to internal variability. J. Clim. 27 (6), 2271–2296.
Diaz, Henry F., 1983. Drought in the United States. J. Appl. Meteorol. Climatol. 22 (1), 3–16.
Fettig, Christopher J., Mortenson, Leif A., Bulaon, Beverly M., Foulk, Patra B., 2019. Tree mortality following drought in the central and southern Sierra Nevada, California, US. For. Ecol. Manag. 432, 164–178.
Francis, Jennifer A., Vavrus, Stephen J., 2012. Evidence linking Arctic amplification to extreme weather in mid-latitudes. Geophys. Res. Lett. 39, 6.
Francis, Jennifer A., Vavrus, Stephen J., 2015. Evidence for a wavier jet stream in response to rapid Arctic warming. Environ. Res. Lett. 10 (1), 014005.
Francis, Jennifer, Vavrus, Stephen, 2021. How is rapid Arctic warming influencing weather patterns in lower latitudes? Arctic Antarct. Alpine Res. 53 (1), 219–220.
Heim, Richard R., 2017. A comparison of the early twenty-first century drought in the United States to the 1930s and 1950s drought episodes. Bull. Am. Meteorol. Soc. 98 (12), 2579–2592.
Jain, Piyush, Flannigan, Mike, 2021. The relationship between the polar jet stream and extreme wildfire events in North America. J. Clim. 34 (15), 6247–6265.
Karl, Thomas R., 1983. Some spatial characteristics of drought duration in the United States. J. Appl. Meteorol. Climatol. 22 (8), 1356–1366.
Knapp, Paul A., Soulé, Peter T., 2017. Spatio-temporal linkages between declining Arctic sea-ice extent and increasing wildfire activity in the western United States. Forests 8 (9), 313.
Liu, Yu, Zhang, Xinjia, Song, Huiming, Cai, Qiufang, Li, Qiang, Zhao, Boyang, Han, Liu, Mei, Ruochen, 2017. Tree-ring-width-based PDSI reconstruction for central Inner Mongolia, China over the past 333 years. Clim. Dynam. 48, 867–879.
Müller, Lena M., Bahn, Michael, 2022. Drought legacies and ecosystem responses to subsequent drought. Global Change Biol. 28 (17), 5086–5103.
Overpeck, Jonathan T., 2013. The challenge of hot drought. Nature 503 (7476), 350–351.
Palmer, Wayne C., 1965. Meteorological Drought, vol. 30. US Department of Commerce, Weather Bureau.
Robeson, Scott M., 2015. Revisiting the recent California drought as an extreme value. Geophys. Res. Lett. 42 (16), 6771–6779.
Screen, James A., Deser, Clara, Simmonds, Ian, Tomas, Robert, 2014. Atmospheric impacts of Arctic sea-ice loss, 1979–2009: separating forced change from atmospheric internal variability. Clim. Dynam. 43, 333–344.
Soulé, Peter T., 1992. Spatial patterns of drought frequency and duration in the contiguous USA based on multiple drought event definitions. Int. J. Climatol. 12 (1), 11–24.
Stahle, David W., Fye, Falko K., Cook, Edward R., Daniel Griffin, R., 2007. Tree-ring reconstructed megadroughts over North America since AD 1300. Climatic Change 83 (1–2), 133–149.
Strzepek, Kenneth, Gary, Yohe, Neumann, James, Boehlert, Brent, 2010. Characterizing changes in drought risk for the United States from climate change. Environ. Res. Lett. 5 (4), 044012.
Swain, Daniel L., Tsiang, Michael, Haugen, Matz, Singh, Deepti, Allison, Charland, Rajaratnam, Bala, Noah, S., Diffenbaugh, 2014. The extraordinary California drought of 2013/2014: character, context, and the role of climate change. Bull. Am. Meteorol. Soc. 95 (9), S3.
Swain, Daniel L., Deepti Singh, Daniel E., Horton, Mankin, Justin S., Ballard, Tristan C., Diffenbaugh, Noah S., 2017. Remote linkages to anomalous winter atmospheric ridging over the northeastern Pacific. J. Geophys. Res. Atmos. 122 (22), 12–194.
Teuling, Adriaan J., 2018. A hot future for European droughts. Nat. Clim. Change 8 (5), 364–365.
Udall, Bradley, Overpeck, Jonathan, 2017. The twenty-first century Colorado River hot drought and implications for the future. Water Resour. Res. 53 (3), 2404–2418.
Wang, Houwen, Gao, Yang, Wang, Yuhang, Sheng, Lifang, 2022. Arctic sea ice modulation of summertime heatwaves over western North America in recent decades. Environ. Res. Lett. 17 (7), 074015.
Williams, A. Park, Benjamin, I. Cook, Smerdon, Jason E., 2022. Rapid intensification of the emerging southwestern North American megadrought in 2020–2021. Nat. Clim. Change 12 (3), 232–234.
Williams, A. Park, Cook, Edward R., Smerdon, Jason E., Cook, Benjamin I., Abatzoglou, John T., Bolles, Kasey, Baek, Seung H., Badger, Andrew M., Livneh, Ben, 2020. Large contribution from anthropogenic warming to an emerging North American megadrought. Science 368 (6488), 314–318.
Williams, A. Park, Richard, Seager, Abatzoglou, John T., Cook, Benjamin I., Smerdon, Jason E., Cook, Edward R., 2015. Contribution of anthropogenic warming to California drought during 2012–2014. Geophys. Res. Lett. 42 (16), 6819–6828.
Wu, Qigang, Kang, Caiyan, Chen, Yibing, Yao, Yonghong, 2023. Significant weakening effects of Arctic Sea ice loss on the summer western hemisphere polar jet stream and troposphere vertical wind shear. Clim. Dynam. 1–23.
Zou, Yufei, Rasch, Philip J., Wang, Hailong, Xie, Zuowei, Zhang, Rudong, 2021. Increasing large wildfires over the western United States linked to diminishing sea ice in the Arctic. Nat. Commun. 12 (1), 6048.